Biochemical and Biophysical Research Communications 434 (2013) 848–853

Contents lists available at SciVerse ScienceDirect

Biochemical and Biophysical Research Communications

journal homepage: www.elsevier.com/locate/ybbrc

Structural characterization of the *Borrelia burgdorferi* outer surface protein BBA73 implicates dimerization as a functional mechanism

Kalvis Brangulis [a,*], Ivars Petrovskis [a], Andris Kazaks [a], Viesturs Baumanis [a,b], Kaspars Tars [a]

[a] Latvian Biomedical Research and Study Centre, Ratsupites 1, LV-1067 Riga, Latvia
[b] University of Latvia, Kronvalda Bulv. 4, LV-1586 Riga, Latvia

ARTICLE INFO

Article history:
Received 26 March 2013
Available online 22 April 2013

Keywords:
Lyme borreliosis
Ixodes ticks
Homologous proteins
Lyme disease therapy
Outer surface proteins

ABSTRACT

Borrelia burgdorferi, which is the causative agent of Lyme disease, is transmitted from infected *Ixodes* ticks to a mammalian host following a tick bite. Upon changing the host organism from an *Ixodes* tick to a warm-blooded mammal, the spirochete must adapt to very different conditions, which is achieved by altering the expression of several genes in response to a changing environment. Recently, considerable attention has been devoted to several outer surface proteins, including BBA73, that undergo dramatic upregulation during the transmission of *B. burgdorferi* from infected *Ixodes* ticks to mammals and that are thought to be important for the establishment and maintenance of the infection. These upregulated proteins could reveal the mechanism of pathogenesis and potentially serve as novel drug targets to prevent the transmission of the pathogenic bacteria.

To promote effective treatments for Lyme disease and to gain better insight into *B. burgdorferi* pathogenesis, we have determined the crystal structure of the upregulated outer surface protein BBA73 at 2.0 Å resolution.

We observed that the BBA73 protein exists as a homodimer both in the crystal and in solution. The monomers interact with their N-terminal α-helices and form a cleft that could potentially serve as a ligand or receptor binding site. To confirm that the protein dimerizes through the interaction of the N-terminal regions, we produced an N-terminal deletion mutant of BBA73 to disrupt dimerization, and we determined the crystal structure of the truncated BBA73 protein at 1.9 Å resolution. The truncated protein did not form a homodimer, and the crystal structure confirmed that the overall fold is identical to that of the native BBA73 protein. Notably, a paralogous protein CspA from *B. burgdorferi* with known crystal structure also forms a homodimer, albeit through an entirely different interaction between the monomers.

1. Introduction

Lyme disease is the most common tick-borne infection caused by the transfer of *Borrelia burgdorferi* from infected *Ixodes* ticks to a mammalian host organism. If not treated by antibiotics or in the case of an inadequate treatment at early stages of the infection, the disease can cause severe neurological symptoms (neuroborreliosis), dermatitis (acrodermatitis chronica atrophicans) or joint inflammation (Lyme arthritis) [1–4].

When an infected *Ixodes* tick bites a mammalian organism and begins to feed, *B. burgdorferi* responds to the mammalian host-specific signals and the occurring changes in temperature, cell density, pH and nutrient level by upregulating the expression of various predominantly surface-exposed proteins, including BBA73, that are thought to be associated with the pathogenesis of *B. burgdorferi* [5–11]. The upregulated proteins are considered to be essential for *B. burgdorferi*, first, to migrate from the midgut of the tick to the salivary glands; secondly, to enter the mammalian host organism; and thirdly, to help the bacteria to disseminate, target to specific tissues and resist the immune response of the vertebrate host organism [12].

Much attention has been directed to the genes residing on the linear plasmid 54 (lp54). lp54 is one of the twelve linear plasmids of *B. burgdorferi* in addition to 9 circular plasmids and the chromosome. Nine genes belonging to the paralogous gene family PFam54 are among the most differentially expressed borrelial genes [6,13] and thus are of particular interest. The *B. burgdorferi* outer surface protein BBA73 is one of the members of the gene family PFam54 and has been shown by several studies to respond to different environmental changes associated with the transfer of the bacteria from *Ixodes* ticks to a mammalian organism. *bba73* has been identified as the second highest temperature-responsive gene through

* Corresponding author. Address: Latvian Biomedical Research and Study Centre, Ratsupites Street 1, LV-1067 Riga, Latvia. Fax: +371 67442407.
E-mail address: kalvis@biomed.lu.lv (K. Brangulis).

0006-291X/$ - see front matter © 2013 Elsevier Inc. All rights reserved.
http://dx.doi.org/10.1016/j.bbrc.2013.04.028

the analysis of all the putative ORFs of *B. burgdorferi* demonstrating increased expression at 35 °C relative to 25 °C [6]. BBA73 is also one of the most upregulated proteins identified after the addition of blood to a spirochete culture at 35 °C for 48 h, thus indicating the potentially important role of BBA73 in the transfer from ticks to the vertebrate host organism [5]. The expression of BBA73 is also increased by a decrease in the pH of the medium from 8.0 to 7.0, which simulates the pH change upon transfer from a tick to a mammalian host [7]. Moreover, BBA73 has been characterized as a potential vaccine candidate based on its antigenicity and conservation among the major Lyme disease-causing borrelial species [14,15]. These observations clearly suggest that the expression of BBA73 is regulated by pH, temperature and host-specific signals, and the protein can be reasonably considered an important constituent of *B. burgdorferi* pathogenesis.

To facilitate the determination of the function of this apparently important protein involved in the pathogenesis of *B. burgdorferi* and to promote the development of novel potential drugs against Lyme disease, we have determined the crystal structure of the outer surface protein BBA73 at 2.0 Å resolution.

2. Materials and methods

2.1. Cloning and expression of BBA73 and BBA73S

The gene encoding the outer surface protein BBA73 of *B. burgdorferi* strain B31 was amplified by PCR from genomic DNA excluding the signal sequence (residues 1–27). The amplified product was ligated into the pETm_11 expression vector (EMBL) encoding an N-terminal 6×His tag followed by a TEV (Tobacco Etch Virus) protease cleavage site. The plasmid was transformed into the *E. coli* strain RR1, and the cells were grown overnight at 37 °C on LB agar plates containing kanamycin. Colonies were inoculated into LB medium containing kanamycin at 37 °C for another 24 h. Plasmid DNA was isolated from the resulting culture and verified by DNA sequencing. For the overexpression of the 6×His-tagged target protein, the plasmid was transformed into *E. coli* BL21(DE3) cells. The cells were grown in modified 2× TYP media (supplemented with kanamycin (10 mg/ml), 133 mM phosphate buffer, pH 7.4, and glucose (4 g/l)) with vigorous agitation at 25 °C until an OD_{600} of 0.8–1.0, induced with 0.2 mM IPTG and grown for an additional 16–20 h. For the truncated protein (BBA73S), the procedure was identical except that the construct was designed to begin at residue Glu87.

2.2. Protein purification and 6×His tag cleavage

E. coli cells were lysed by sonication, and the cell debris was removed by centrifugation. The recombinant proteins BBA73 and BBA73S containing 6×His tags were purified using affinity chromatography on a Ni–NTA agarose (Qiagen, Germany) column followed by a buffer exchange to 10 mM Tris–HCl, pH 8.0, using an Amicon centrifugal filter unit (Millipore).

A recombinant TEV protease was added to BBA73 and BBA73S to remove the 6×His tag, and the reaction was incubated overnight at room temperature. The protease, the digested 6×His tag and the remnants of uncleaved protein were removed using an additional round of Ni–NTA chromatography. Both proteins were further purified using ion-exchange chromatography on a Mono Q 5/50 GL column (GE Healthcare).

2.3. Mass spectrometry

The state of the protein in the crystals was analyzed using MALDI-TOF mass spectrometry and compared with an identical protein batch used for crystallization. The obtained protein crystals were dissolved in 10 mM Tris–HCl, pH 8.0, and 1 μl of protein (11 mg/ml in 10 mM Tris–HCl, pH 8.0) was mixed with 1 μl of 0.1% TFA and 1 μl of matrix solution containing 15 mg/ml 2,5-dihydroxyacetophenone in 20 mM ammonium citrate and 75% ethanol. An identical procedure was performed on the batch of protein used for crystallization, and 1 μl of the obtained mixture was loaded on the target plate, dried and analyzed using a Bruker Daltonics Autoflex mass spectrometer.

2.4. Estimation of the multimeric state using size exclusion chromatography

The purified protein sample at a concentration of 4 mg/ml in 10 mM Tris–HCl, pH 8.0, and 0.2 M, 0.5 M or 1 M NaCl was loaded onto a prepacked Superdex 200 10/300 GL column (Amersham Biosciences). The column was preequilibrated with an identical buffer and run at a flow rate of 0.7 ml/min. Bovine serum albumin (67 kDa), ovalbumin (43 kDa) and chymotrypsinogen A (25 kDa) were used as MW reference standards.

2.5. Crystallization of the native and truncated protein

Crystallization was performed using the sitting drop vapor diffusion method in 96-well plates by mixing 1 μl of protein with an equal volume of precipitant solution. Sparse-matrix screens consisting of 96 reagents were used for the initial screening of crystallization conditions for BBA73, and protein crystals were obtained in 12% PEG 20,000 and 0.1 M MES, pH 6.5, from the Structure Screen 1 & 2 (Molecular Dimensions Ltd., UK). The conditions were further optimized, and needle-shaped crystals of BBA73 were obtained in 14% PEG 3350, 0.1 M HEPES, pH 7.0, and 0.05 M NaH_2PO_4. The BBA73S protein was crystallized in 18% PEG 3350 and 0.1 M MES, pH 6.5, resulting in a different, tetragonal crystal form. As a cryoprotectant, the mother liquor with 25% glycerol was used in both cases, and crystals were flash-frozen in liquid nitrogen.

2.6. Data collection and structure determination

Diffraction data for the native and truncated proteins were collected at the MAX-lab beamlines I911–3 and I911–2 (Lund, Sweden). Reflections were indexed and scaled using MOSFLM [16] and SCALA [17] from the CCP4 suite [18]. Initial phases for BBA73 were obtained by molecular replacement using Phaser [19] and the crystal structure of the paralogous protein BBA64 as a search model (22% sequence identity, PDB entry 4ALY). For BBA73S, the crystal structure of BBA73 was used as a search model. For BBA73, molecular replacement was followed by automatic model building using BUCCANEER [20], and for both structures, the models were improved by manual rebuilding in COOT [21]. Crystallographic refinement was performed using REFMAC5 [22]. Water molecules were picked automatically in COOT and inspected manually.

A summary of the data collection, refinement and validation statistics for BBA73 and BBA73S is provided in Table 1.

3. Results and discussion

3.1. Overall crystal structure of BBA73 and BBA73S

The protein model for full-length BBA73 was built for residues 71–287 and for residues 87–287 of the truncated protein (BBA73S). The signal sequence of BBA73 (residues 1–27) was already excluded from the expressed protein, and residues 28–70 at the N-terminus of BBA73 were not observed in the electron density map. The electron density for the C-terminal residues 288–296 in

Table 1
Statistics for data and structure quality.

Dataset	Native BBA73	Truncated BBA73
Space group	P 2_12_12	P 4_32_12
Unit cell dimensions		
A (Å)	153.63	74.34
B (Å)	47.10	74.34
C (Å)	34.50	95.62
Wavelength (Å)	1.0000	1.0408
Resolution (Å)	40.15–2.09	23.03–1.88
Highest resolution bin (Å)	2.20–2.09	1.98–1.88
No. of reflections	216455	106455
No. of unique reflections	15642	21966
Completeness (%)	99.9 (99.8)	98.6 (99.7)
R_{merge}	0.07 (0.36)	0.06 (0.49)
I/σ (I)	22.8 (6.8)	17.0 (3.1)
Multiplicity	13.8 (12.2)	4.8 (4.8)
Refinement		
R_{work}	0.215 (0.231)	0.204 (0.271)
R_{free}	0.244 (0.298)	0.235 (0.340)
Average B-factor (Å^2)		
Overall	32.0	23.9
From Wilson plot	29.1	29
No. of atoms		
Protein	1795	1667
Ligand	0	0
Water	87	84
RMS deviations from ideal		
Bond lengths (Å)	0.011	0.009
Bond angles (°)	1.382	1.124
Ramachandran outliers (%)		
Residues in most favored regions (%)	98.15	98.02
Residues in allowed regions (%)	1.85	1.98
Outliers (%)	0.00	0.00

*Values in parentheses are for the highest resolution bin.

both BBA73 and BBA73S were largely uninterpretable, and these residues were therefore excluded from the final model. To determine whether the N-terminal residues 28–70 in BBA73 are disordered or absent in the crystal, we analyzed the crystallized material using mass spectrometry. The results revealed that residues 28–49, although present in the purified protein, are absent in the crystallized material likely due to a proteolytic susceptibility similar to that reported for the homologous proteins BBA64 and CspA [23]. In contrast, residues 50–70, although present in the crystal, could not be observed in the electron density map likely due to the flexible nature of the N-terminus of the protein, which is most likely unstructured and serves as a linker between the structured domain and the cell surface.

The crystal structure of the BBA73 monomer consists of seven α-helices, which are from 5 to 28 residues long, that are connected by loops of different lengths, and the overall fold is similar to the homologous proteins BBA64 and CspA (Fig. 1A).

3.2. PFam54 family members and the dimerization of BBA73

The amino acid sequence identity among the 11 members (9 members located on lp54) of the PFam54 paralogous gene family of *B. burgdorferi* varies from 17% to 60%. The functions of the paralogous protein family members are thought to be different, as reported by several studies indicating that the expression level, timing and the target receptors/ligands differ substantially among the PFam54 family members [24,25]. Although all of these proteins are thought to be related to the pathogenesis of *B. burgdorferi,* the exact function has been established only for one protein, CspA, from the PFam54 family. CspA is a complement regulator factor H and factor H-like protein-1 (FHL-1) binding protein, and thus, it assists the bacteria to resist the host immune response. CspA is the only PFam54 member that is known to bind complement regulators, as verified by several studies [26–29]. Previously, crystal structures have been determined for two members of the PFam54 family: the aforementioned CspA and an outer surface protein, BBA64. BBA64 plays an essential role in the transfer of *B. burgdorferi* from infected *Ixodes* ticks to a mammalian host organism after a tick bite, although the exact ligand or receptor is not known [30,31]. The major difference between CspA and BBA64 as observed from the crystal structures of both proteins is the different orientation of the C-terminal α-helix, which, in the case of BBA64, does not form a stalk-like extension protruding outwards from the globular protein fold but instead bends backwards to form a compact globular domain [23]. The studies on C-terminal deletion mutants of CspA have indicated that the C-terminal α-helix is essential for the binding of the complement regulators, although additional regions have also been determined to be associated with the binding of the complement factor H and FHL-1 [29,32,33]. The importance of the C-terminal region became evident when it was shown that the C-terminal α-helix of CspA is involved in dimerization by burying an extensive 2240.9 Å^2 surface area at the dimer interface. Dimerization of CspA has been proposed to be important for its function, and it is thought that the complement factor H and FHL-1 bind at the cleft between the monomers (Fig. 1B) [23,29,34].

The crystal structure of BBA73 revealed that the overall protein fold is more similar to the homologous protein BBA64 because the C-terminal α-helix does not form a stalk-like extension as was observed for CspA (Fig. 1C). However, using size exclusion chromatography, we determined that BBA73 forms a stable homodimer in solution. A closer inspection of the BBA73 crystal structure and the prediction of possible interfaces using the PISA software (Protein Interfaces, Surfaces and Assemblies prediction tool) revealed that the N-terminal α-helices of two monomers interact with each other and form a 600 Å^2 contact area in which several large hydrophobic residues (2 phenylalanines and 3 isoleucines from each subunit) are buried. Because a moderate 600 Å^2 contact area cannot be regarded as a reliable dimerization interface, we wished to confirm our assumption that the N-terminal α-helix is indeed sufficient and necessary for dimerization in solution and that the observed interaction is not merely a crystal contact. We produced an N-terminal deletion mutant of BBA73 (named BBA73S in this study) excluding the first 16 residues from α-helix A (residues 71–86) that were observed to be involved in the dimerization. The crystal structure of the truncated protein BBA73S revealed that the overall protein structure is identical to BBA73, demonstrating that the deletion of the N-terminal residues from α-helix A does not affect the overall fold of the molecule. Size exclusion chromatography indicated that BBA73S eluted as a monomer, confirming that the N-terminal α-helix is indeed necessary for dimerization (Fig. 1A). As previously mentioned, BBA73 appeared to contain a slightly longer N-terminal region than that observed for the homologous proteins CspA and BBA64, and approximately 20 residues from α-helix A are found in the dimerization interface (residues 71–90). Additionally, the secondary structure prediction software PSIPRED v3.0 [35] predicted with a high confidence that the N-terminal α-helix could be approximately 11 residues longer than that in the solved crystal structure. Therefore, the actual interaction surface between the monomers in solution could be even larger and could already begin from residue Leu61. This prediction would be consistent with the crystal structure of BBA73, although electron density was not observed for this region likely due to the flexible nature of the N-terminal region of the molecule.

The exact reason for BBA73 dimerization remains unknown, but the cleft between the monomers might serve as a binding surface for a potential ligand/receptor.

To further explore the characteristics of the BBA73 dimer, the electrostatic surface potential for BBA73 was analyzed. The

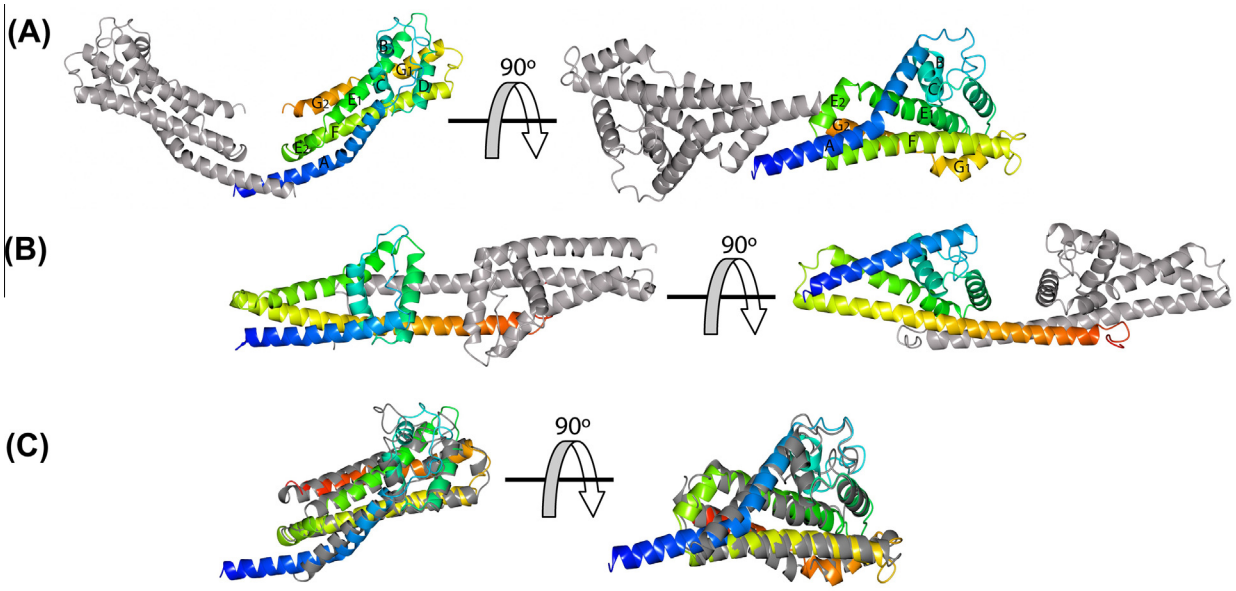

Fig. 1. Differences in the crystal structures of the homologous proteins BBA73, CspA and BBA64. (A) Homodimer of BBA73 formed by the interaction of the N-terminal α-helices as viewed from two different angles rotated by 90 degrees in the horizontal plane. (B) Homodimer of the homologous protein CspA formed by the interaction of the C-terminal α-helices viewed in an identical orientation as for BBA73. (C) Superimposed crystal structures of BBA73 (colored molecule) and BBA64 (gray) monomers oriented at different angles, as shown for the BBA73 dimers. In the dimers, one molecule of the dimer is shown in rainbow representation colored in blue at the N-terminus and gradually switching to red at the C-terminus, whereas the other monomer is colored gray. (For interpretation of the references to color in this figure legend, the reader is referred to the web version of this article.)

analysis of the dimer revealed that the cleft between the monomers is predominately negatively charged, suggesting that this negative charge could be necessary for the binding of a positively charged ligand/receptor (Fig. 2). In contrast, the bottom of the dimer molecule is predominately positively charged, which could possibly contribute to the protein function as well.

4. Residue conservation in the homologous proteins

A structure-based sequence alignment comparing BBA73 with other members of the homologous protein family PFam54 with known crystal structures is shown in Fig. 3. The sequence identity among the homologous proteins ranges from 18% between BBA73 and CspA to 22% between BBA73 and BBA64. Structure-based sequence comparison revealed several segments in the crystal structures of the three homologous proteins that were conserved among all of the members. One of the most conserved regions among all three members is located in α-helices C and D (as defined in BBA73). Structural comparison reveals that the conserved residues (residues Arg145, Tyr148, Ser150, Leu151, Ile158, Leu161, Ile164 and Leu165, as numbered in BBA73) are facing the hydrophobic core of the proteins and are apparently necessary for the stabilization of the fold in this region. One partially buried conserved salt bridge, which links Arg145 and Glu194, is observed in all of the structures. Presumably, the salt bridge plays an important role in the stabilization of the fold and the positioning of α-helices C and E (as designated in BBA73). Although this region of the molecule is associated with the potential binding site in CspA and the sequence alignment indicates high conservation among the three homologous proteins, actually the surface-exposed residues that could be involved in ligand/receptor binding differ among the homologous proteins, which may reflect the diverse functions of the three proteins. There are also conserved residues in α-helices E and G of BBA73 that correspond to α-helices D and E, respectively, in BBA64 and CspA (residues Ile189, Gln190, Glu194 and Tyr245, as numbered in BBA73) all of which also point toward the protein core and are located in nearly identical positions in all of the protein structures, which suggests their role in the preservation of the overall fold.

There are only a few residues (Glu100, Gln104, Lys236 and Asn248, as numbered in BBA73) that are exposed to the surface of the protein molecules and are conserved among the homologs. None of the four conserved residues are located near the cleft between the monomers that is suggested as a potential binding site.

5. Accession numbers

The coordinates and structure factors for BBA73 and the N-terminal truncation mutant of BBA73 have been deposited in the Protein Data Bank with the accession numbers 4AXZ and 4B2F.

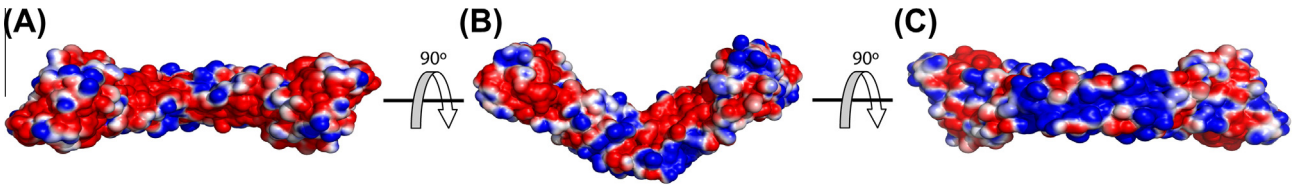

Fig. 2. Electrostatic surface potential of the BBA73 dimer. The homodimer is shown in three different orientations, each rotated by 90 degrees. The electrostatic potential (red, negative; blue, positive) was calculated using APBS [41], and the surface contour level is set to −1 kT/e (red) and +1 kT/e (blue). (For interpretation of the references to color in this figure legend, the reader is referred to the web version of this article.)

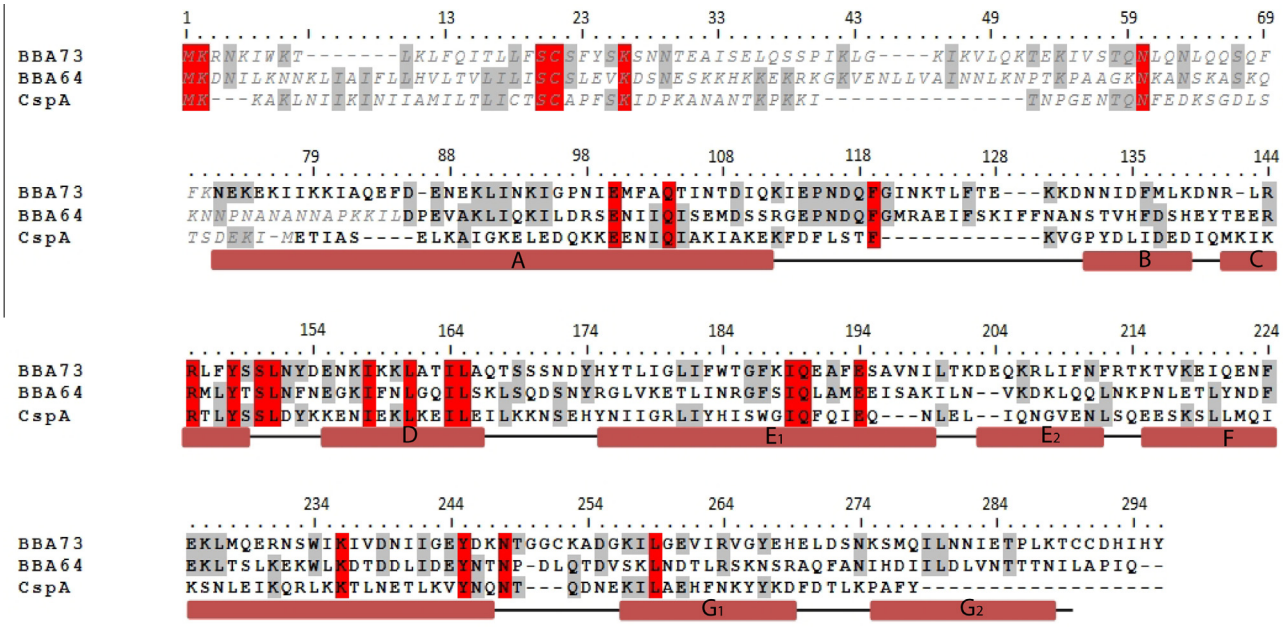

Fig. 3. Structure-based sequence alignment of BBA73 and the homologous proteins BBA64 and CspA. Residues not observed in the electron density map for BBA73, BBA64 and CspA are indicated in italics and colored gray. Conserved residues of all three homologous proteins are colored red, but residues conserved between any two members are colored in gray. The secondary structure is represented for BBA73 below the alignment sequence as cylinders for α-helices and as lines for loop regions. The numbering above the alignment is shown for BBA73. (For interpretation of the references to color in this figure legend, the reader is referred to the web version of this article.)

Acknowledgments

This work was supported by the ESF Grant 1DP/1.1.1.2.0/09/APIA/VIAA/150 and Latvian Council of Science Nr. 10.0029.3. We thank Dr. Gunter Stier and Dr. Huseyin Besir from the EMBL for providing the expression vector pETm-11. The staff at the MAX-lab synchrotron is acknowledged for their professional support during the data collection.

References

[1] R.R. Mullegger, M. Glatz, Skin manifestations of Lyme borreliosis: diagnosis and management, Am. J. Clin. Dermatol. 9 (2008) 355–368.
[2] A.R. Pachner, D. Cadavid, G. Shu, D. Dail, S. Pachner, E. Hodzic, S.W. Barthold, Central and peripheral nervous system infection, immunity, and inflammation in the NHP model of Lyme borreliosis, Ann. Neurol. 50 (2001) 330–338.
[3] A.C. Steere, L. Glickstein, Elucidation of Lyme arthritis, Nat. Rev. Immunol. 4 (2004) 143–152.
[4] J.J. Halperin, Neurologic manifestations of Lyme disease, Curr. Infect. Dis. Rep. 13 (2011) 360–366.
[5] R. Tokarz, J.M. Anderton, L.I. Katona, J.L. Benach, Combined effects of blood and temperature shift on Borrelia burgdorferi gene expression as determined by whole genome DNA array, Infect. Immun. 72 (2004) 5419–5432.
[6] C. Ojaimi, C. Brooks, S. Casjens, P. Rosa, A. Elias, A. Barbour, A. Jasinskas, J. Benach, L. Katona, J. Radolf, M. Caimano, J. Skare, K. Swingle, D. Akins, I. Schwartz, Profiling of temperature-induced changes in Borrelia burgdorferi gene expression by using whole genome arrays, Infect. Immun. 71 (2003) 1689–1705.
[7] J.A. Carroll, R.M. Cordova, C.F. Garon, Identification of 11 pH-regulated genes in Borrelia burgdorferi localizing to linear plasmids, Infect. Immun. 68 (2000) 6677–6684.
[8] T.E. Angel, B.J. Luft, X. Yang, C.D. Nicora, D.G. Camp 2nd, J.M. Jacobs, R.D. Smith, Proteome analysis of Borrelia burgdorferi response to environmental change, PLoS One 5 (2010) e13800.
[9] C.S. Brooks, P.S. Hefty, S.E. Jolliff, D.R. Akins, Global analysis of Borrelia burgdorferi genes regulated by mammalian host-specific signals, Infect. Immun. 71 (2003) 3371–3383.
[10] K.J. Indest, R. Ramamoorthy, M. Sole, R.D. Gilmore, B.J. Johnson, M.T. Philipp, Cell-density-dependent expression of Borrelia burgdorferi lipoproteins in vitro, Infect. Immun. 65 (1997) 1165–1171.
[11] A.T. Revel, A.M. Talaat, M.V. Norgard, DNA microarray analysis of differential gene expression in Borrelia burgdorferi, the Lyme disease spirochete, Proc. Natl. Acad. Sci. USA 99 (2002) 1562–1567.
[12] M.R. Kenedy, T.R. Lenhart, D.R. Akins, The role of Borrelia burgdorferi outer surface proteins, FEMS Immunol. Med. Microbiol. 66 (2012) 1–19.
[13] S. Casjens, N. Palmer, R. van Vugt, W.M. Huang, B. Stevenson, P. Rosa, R. Lathigra, G. Sutton, J. Peterson, R.J. Dodson, D. Haft, E. Hickey, M. Gwinn, O. White, C.M. Fraser, A bacterial genome in flux: the twelve linear and nine circular extrachromosomal DNAs in an infectious isolate of the Lyme disease spirochete Borrelia burgdorferi, Mol. Microbiol. 35 (2000) 490–516.
[14] A. Poljak, P. Comstedt, M. Hanner, W. Schuler, A. Meinke, B. Wizel, U. Lundberg, Identification and characterization of Borrelia antigens as potential vaccine candidates against Lyme borreliosis, Vaccine 30 (2012) 4398–4406.
[15] E. Wywial, J. Haven, S.R. Casjens, Y.A. Hernandez, S. Singh, E.F. Mongodin, C.M. Fraser-Liggett, B.J. Luft, S.E. Schutzer, W.G. Qiu, Fast, adaptive evolution at a bacterial host-resistance locus: the PFam54 gene array in Borrelia burgdorferi, Gene 445 (2009) 26–37.
[16] A.G. Leslie, The integration of macromolecular diffraction data, Acta Crystallogr. D Biol. Crystallogr. 62 (2006) 48–57.
[17] P. Evans, Scaling and assessment of data quality, Acta Crystallogr. D Biol. Crystallogr. 62 (2006) 72–82.
[18] M.D. Winn, C.C. Ballard, K.D. Cowtan, E.J. Dodson, P. Emsley, P.R. Evans, R.M. Keegan, E.B. Krissinel, A.G. Leslie, A. McCoy, S.J. McNicholas, G.N. Murshudov, N.S. Pannu, E.A. Potterton, H.R. Powell, R.J. Read, A. Vagin, K.S. Wilson, Overview of the CCP4 suite and current developments, Acta Crystallogr. D Biol. Crystallogr. 67 (2011) 235–242.
[19] A.J. McCoy, R.W. Grosse-Kunstleve, P.D. Adams, M.D. Winn, L.C. Storoni, R.J. Read, Phaser crystallographic software, J. Appl. Crystallogr. 40 (2007) 658–674.
[20] K. Cowtan, The Buccaneer software for automated model building. 1. Tracing protein chains, Acta Crystallogr. D Biol. Crystallogr. 62 (2006) 1002–1011.
[21] P. Emsley, K. Cowtan, Coot: model-building tools for molecular graphics, Acta Crystallogr. D Biol. Crystallogr. 60 (2004) 2126–2132.
[22] G.N. Murshudov, A.A. Vagin, E.J. Dodson, Refinement of macromolecular structures by the maximum-likelihood method, Acta Crystallogr. D Biol. Crystallogr. 53 (1997) 240–255.
[23] F.S. Cordes, P. Roversi, P. Kraiczy, M.M. Simon, V. Brade, O. Jahraus, R. Wallis, C. Skerka, P.F. Zipfel, R. Wallich, S.M. Lea, A novel fold for the factor H-binding protein BbCRASP-1 of Borrelia burgdorferi, Nat. Struct. Mol. Biol. 12 (2005) 276–277.
[24] R.D. Gilmore Jr., R.R. Howison, V.L. Schmit, A.J. Nowalk, D.R. Clifton, C. Nolder, J.L. Hughes, J.A. Carroll, Temporal expression analysis of the Borrelia burgdorferi paralogous gene family 54 genes BBA64, BBA65, and BBA66 during persistent infection in mice, Infect. Immun. 75 (2007) 2753–2764.
[25] R.D. Gilmore Jr., R.R. Howison, V.L. Schmit, J.A. Carroll, Borrelia burgdorferi expression of the bba64, bba65, bba66, and bba73 genes in tissues during persistent infection in mice, Microb. Pathog. 45 (2008) 355–360.
[26] P. Kraiczy, E. Rossmann, V. Brade, M.M. Simon, C. Skerka, P.F. Zipfel, R. Wallich, Binding of human complement regulators FHL-1 and factor H to CRASP-1 orthologs of Borrelia burgdorferi, Wien Klin Wochenschr. 118 (2006) 669–676.
[27] P. Kraiczy, C. Skerka, M. Kirschfink, V. Brade, P.F. Zipfel, Immune evasion of Borrelia burgdorferi by acquisition of human complement regulators FHL-1/reconectin and Factor H, Eur. J. Immunol. 31 (2001) 1674–1684.
[28] R. Wallich, J. Pattathu, V. Kitiratschky, C. Brenner, P.F. Zipfel, V. Brade, M.M. Simon, P. Kraiczy, Identification and functional characterization of

complement regulator-acquiring surface protein 1 of the Lyme disease spirochetes Borrelia afzelii and Borrelia garinii, Infect. Immun. 73 (2005) 2351–2359.

[29] P. Kraiczy, C. Hanssen-Hubner, V. Kitiratschky, C. Brenner, S. Besier, V. Brade, M.M. Simon, C. Skerka, P. Roversi, S.M. Lea, B. Stevenson, R. Wallich, P.F. Zipfel, Mutational analyses of the BbCRASP-1 protein of Borrelia burgdorferi identify residues relevant for the architecture and binding of host complement regulators FHL-1 and factor H, Int. J. Med. Microbiol. 299 (2009) 255–268.

[30] F.S. Cordes, P. Kraiczy, P. Roversi, C. Skerka, M. Kirschfink, M.M. Simon, V. Brade, E.D. Lowe, P. Zipfel, R. Wallich, S.M. Lea, Crystallization and preliminary crystallographic analysis of BbCRASP-1, a complement regulator-acquiring surface protein of Borrelia burgdorferi, Acta Crystallogr. D Biol. Crystallogr. 60 (2004) 929–932.

[31] R.D. Gilmore Jr., R.R. Howison, G. Dietrich, T.G. Patton, D.R. Clifton, J.A. Carroll, The bba64 gene of Borrelia burgdorferi, the Lyme disease agent, is critical for mammalian infection via tick bite transmission, Proc. Natl. Acad. Sci. USA 107 (2010) 7515–7520.

[32] J.V. McDowell, M.E. Harlin, E.A. Rogers, R.T. Marconi, Putative coiled-coil structural elements of the BBA68 protein of Lyme disease spirochetes are required for formation of its factor H binding site, J. Bacteriol. 187 (2005) 1317–1323.

[33] P. Herzberger, C. Siegel, C. Skerka, V. Fingerle, U. Schulte-Spechtel, B. Wilske, V. Brade, P.F. Zipfel, R. Wallich, P. Kraiczy, Identification and characterization of the factor H and FHL-1 binding complement regulator-acquiring surface protein 1 of the Lyme disease spirochete Borrelia spielmanii sp. nov, Int. J. Med. Microbiol. 299 (2009) 141–154.

[34] F.S. Cordes, P. Kraiczy, P. Roversi, M.M. Simon, V. Brade, O. Jahraus, R. Wallis, L. Goodstadt, C.P. Ponting, C. Skerka, P.F. Zipfel, R. Wallich, S.M. Lea, Structure-function mapping of BbCRASP-1, the key complement factor H and FHL-1 binding protein of Borrelia burgdorferi, Int. J. Med. Microbiol. 296 (Suppl. 40) (2006) 177–184.

[35] D.T. Jones, Protein secondary structure prediction based on position-specific scoring matrices, J. Mol. Biol. 292 (1999) 195–202.